

## Petrography and Provenance of Basement Clasts and Clast Variability in CRP-3 Drillcore (Victoria Land Basin, Antarctica)

S. SANDRONI\* & F. TALARICO

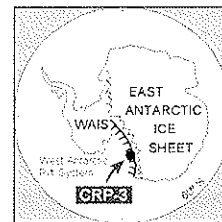
Dipartimento di Scienze della Terra, Università di Siena, via del Laterano 8, 53100 Siena - Italy

Received 30 November 2000; accepted in revised form 2 November 2001

**Abstract** - Distribution patterns and petrographical and mineral chemistry data are described for the most representative basement lithologies occurring as clasts in the c. 824 m thick Tertiary sedimentary sequence at the CRP-3 drillsite. These are granule to boulder grain size clasts of igneous and metamorphic rocks.

Within the basement clast assemblage, granitoid pebbles are the predominant lithology. They consist of dominant grey biotite-bearing monzogranite, pink biotite-hornblende monzogranite, and biotite-bearing leucomonzogranite. Minor lithologies include: actinolite-bearing leuconalite, microgranite, biotite-hornblende quartz-monzonitic porphyry, and foliated biotite leucomonzogranite. Metamorphic clasts include rocks of both granitic and sedimentary derivation. They include mylonitic biotite orthogneiss, with or without garnet, muscovite-bearing quartzite, sillimanite-biotite paragneiss, biotite meta-sandstone, biotite-spotted schist, biotite-calcite-clinoamphibole meta-feldspathic arenite, biotite-calcite-clinozoisite meta-siltstone, biotite-clinoamphibole meta-marl, and graphite-bearing marble.

As in previous CRP drillcores, the ubiquitous occurrence of biotite±hornblende monzogranite pebbles is indicative of a local provenance, closely mirroring the dominance of these lithologies in the on-shore basement, where the Cambro-Ordovician Granite Harbour Intrusive Complex forms the most extensively exposed rock unit.



### INTRODUCTION

Drilling at CRP-3 provided an almost continuous core through c. 824 m of Cenozoic sedimentary strata on the western edge of the Victoria Land Basin, at the western margin of the Ross Sea continental shelf (Cooper et al., 1994, and ref. therein). The on-shore region, part of the southern Victoria Land sector of the Transantarctic Mountains, shows a late Precambrian-Early Palaeozoic crystalline basement comprised of granitoids (Granite Harbour Intrusive Complex) and metamorphic rocks (Koettlitz Group) (Stump, 1995, and ref. therein). This crystalline basement is overlain by a quartzose sedimentary cover of Devonian to Triassic age (Beacon Supergroup), both intruded by dolerite sills and dykes of Jurassic age (Ferrari Supergroup). Lavas and pyroclastic rocks (Kirkpatrick Basalt) are another significant component of the Ferrari Supergroup in the region to the west of Cape Roberts, whereas Cenozoic alkalic volcanics of the McMurdo Volcanic Group crop out to the east and south of McMurdo Sound.

Drilling at CRP-3 (Cape Roberts Science Team, 2000) was performed c. 12 km east of Cape Roberts, c. 2 000 m inboard of CRP-1, the first drillsite of the Cape Roberts Project (Cape Roberts Science Team, 1998a, 1998b, 1998c & 1998d). The objectives and background of the project, as well as the stratigraphy,

depositional and tectonic features of the recovered strata, are reported and described in Cape Roberts Science Team (2000). This paper presents distribution data on the coarse clast population throughout the CRP-3 core, and petrographical and mineral chemistry data on the most representative plutonic and metamorphic lithologies occurring as pebble- to boulder-size clasts. In agreement with provenance inferences reported for previous CRP boreholes (Talarico & Sandroni, 1998; Talarico et al., 2000), the new data provide further evidence of a local provenance for basement clasts and their derivation from the locally exposed Granite Harbour Intrusive Complex.

### PRELIMINARY PETROGRAPHICAL CHARACTERISATION OF CRP-3 BASEMENT CLASTS AND CLAST VARIABILITY

The persistent supply of basement-derived pebbles and dominance of glacial sedimentary facies throughout most of the recovered sedimentary strata at the western edge of the Victoria Land Basin has already been documented by previous boreholes (CIROS-1, MSSTS) in the McMurdo Sound area (Barrett et al., 1986, 1987; George, 1989; Hambrey et al., 1989). Dominant undeformed or foliated biotite ±

\*Corresponding author (sandroni@unisi.it)

hornblende monzogranites were found in both the CRP-1 core (Talarico & Sandroni, 1998) and the CRP-2/2A core (Talarico et al., 2000).

Preliminary investigations on CRP-3 basement clasts (Cape Roberts Science Team, 2000) showed that all the major rock units exposed in the on-shore region presently facing the CRP drillsite area are potential sources of detritus to the CRP-3 site. In the c. 824 m thick Cenozoic section, 27 669 clasts, ranging in dimension from granule to boulder grade, were logged and counted on the basis of both approximate grain-size and lithology. The total number of clasts *per* unit length shows major variations from 0-10 counts *per* metre for mud- or sand-rich intervals (*e.g.* Litostratigraphic sub-Unit [LSU] 1.3) to >150 counts *per* metre for diamictite units (*e.g.* LSU 2.1) and conglomerate units (*e.g.* LSU 12.3, Tab. 1). Sharp variations across lithological boundaries are commonly present, as well as within-unit fluctuations.

Five main lithological groups were distinguished among the clasts. Their main petrographical features and clast dimensions can be summarised as follows:

1) *Granitoids*. These consist mainly of biotite±hornblende monzogranites, with minor occurrence of leucotonalite, mostly represented within the granule class (fragments of quartz and/or pink feldspar crystals, and lithic fragments);

2) *Dolerites*. Generally medium-grained and fresh (Pompilio et al., this volume). Only a few, scattered occurrences of highly altered granules and small pebbles were noted in LSU 3.1, 5.1, 6.1, 11.1, 12.4, 13.1 and at the bottom of LSU 15.2. Dolerite clasts show the widest range in size, ranging from granule to boulders as much as 2 m across;

3) *Sedimentary rocks*. These include at least four lithological types (Cape Roberts Science Team, 2000): quartz-arenite, poorly- to moderately-sorted sandstone, grey to black siltstone, and coal; these clasts mainly belong to the small-pebble class, apart from coal fragments which occur mainly as granules;

4) *Volcanic and sub-volcanic rocks*. This group includes very fine-grained dolerite, non-vesicular basalt and amygdule-bearing altered basalt (Pompilio et al., this volume). All of these varieties mainly form granules to small pebbles;

5) *Metamorphic rocks*. A variety of metamorphic rocks, ranging from basement rocks such as orthogneiss, paragneiss and marble, to low-grade metasedimentary rocks of various origins, are represented in this lithological group. All of these rock types occur only as small pebbles.

The distribution of these different lithological types is shown in Appendix 1. Both granitoids and

Tab. 1 - Petrographical classification and mineral assemblages of representative samples of basement clasts from the Cenozoic section of the CRP-3 borehole.

Sample code	Top (mbsf)	Clast shape	Approximate size (cm)	Lithology	Mineral assemblage	Main petrographical features	Inferred provenance	LSU
TAL2	30.61	subrounded	2x1x0.5	grey Bt-bearing monzogranite	Pl (34%), Kfs (33%), Qtz (33%), Ms (s), Chl (s), Ep (s), Opm (s)	equigranular (fine-grained), hypidiomorphic	G.H.I.C.	1.2
TAL4	43.57	rounded	0.5x0.5x0.5	pink Bt-Hbl bearing monzogranite	Qtz (34%), Kfs (32%), Pl (31%), Bt (2%), green Hbl (1%), Ms (s), Chl (s), Prh (s), Ep (s), Ttn (s), Aln (t), Ap (t), Zrn/Mnz (t), Opm (t)	equigranular (medium-grained), hypidiomorphic	G.H.I.C.	1.2
TAL5	50.25	subrounded	2x1x1	Act-bearing leucotonalite	Pl (75%), Qtz (25%), Aln (t), Act (t), Crb (s), Ms (s), Chl (s), Opm (t), Ap (t)	inequigranular (fine- to medium-grained), hypidiomorphic, altered	G.H.I.C.	1.2
TAL11	107.32	rounded	2.5x1x1	Bt-bearing leucomonzogranite	Pl (36%), Kfs (33%), Qtz (30%), Bt (1%), Ms (s), Chl (s), Ep (s), Opm (s)	inequigranular (fine- to medium-grained), hypidiomorphic, slightly foliated fabric, strongly altered	G.H.I.C.	2.2
TAL16	132.19	subangular	2x1x0.5	Ms-bearing quartzite	Qtz, Ms, Tur, Opm, Zrn/Mnz	equigranular (fine-grained), subpolygonal granoblastic texture, slightly foliated	K.G.	3.1
TAL22	166.18	subrounded	1x1.5x0.5	nylonitic Grt-Bt leuco-orthogneiss	Qtz, Pl, Mc, Bt, Ms (s), Chl (s), Opm (s), Grt, Tur	heterogranular (fine- to medium-grained), gneissic texture (mm-scale compositional layering) with mm-sized feldspar porphyroclasts	K.G.	5.1
TAL23	168.73	rounded	4x3x3	Bt-bearing monzogranite	Mc (38%), Qtz (35%), Pl (26%), Bt (1%), Ms (s), Chl (s), Cal (s), Opm (t), Rt (s), Zrn/Mnz (t)	inequigranular (fine- to coarse-grained), hypidiomorphic, slightly altered	G.H.I.C.	5.1
TAL26	176.03	rounded	3.5x5x3	pink Bt-Hbl monzogranite	Kfs (33%), Qtz (32%), Bt (3.5%), green Hbl (0.5%), Ms (s), Chl (s), Opm (t), Aln (t), Zrn/Mnz (t), Ap (t)	inequigranular (fine- to coarse-grained), porphyritic, mm-sized feldspar phenocrysts and fine-grained allotropic groundmass	G.H.I.C.	5.2
TAL27	178.41	subrounded	2x1.5x0.5	pink Hbl-Bt monzogranite	Kfs (35%), Pl (32%), Qtz (31%), green Hbl (1.2%), Bt (0.8%), Ms (t), Chl (s), Ep (s), Prh (s), Aln (t), Opm (t), Zrn/Mnz (t), Ap (t)	equigranular (medium-grained), hypidiomorphic, altered	G.H.I.C.	5.3
TAL36	216.98	subrounded	25x6x3	grey Bt-bearing leucomonzogranite	Qtz (37%), Kfs (32%), Pl (30%), Bt (1%), Ms (s), Chl (s), Prh (s), Opm (t), Zrn/Mnz (t), Ap (t)	inequigranular (fine- to medium-grained), hypidiomorphic, sub-solidus deformational microstructures, altered	G.H.I.C.	7.2
TAL41	227.98	rounded	2.5x2x1	Bt-bearing meta-quartz arenite	Qtz, Bt, Chl (s), Zrn, Opm	equigranular (fine-grained), interlobate granoblastic	B.S.? (contact metamorphosed?)	7.2
TAL42	231.78	rounded	1.5x1.5x0.5	nylonitic Bt leuco-orthogneiss	Qtz, Pl, Kfs, Ms (s), Bt, Chl (s), Opm	heterogranular (fine- to medium-grained), gneissic texture (mm-scale compositional layering) with mm-sized feldspar porphyroclasts, strongly altered	K.G.	7.2
TAL43	256.38	angular	3x1.5x0.5	pink Hbl-Bt monzogranite	Qtz (33%), Kfs (31%), Pl (31%), green Hbl (3%), Bt (2%), Ms (s), Chl (s), Prh (s), Ep (s), Ttn (s), Aln (t), Ap (t), Zrn/Mnz (t), Opm (t)	inequigranular (fine- to medium-grained), hypidiomorphic, slightly altered	G.H.I.C.	7.2
TAL57	335.31	subrounded	4x2.5x1	pink Bt-Hbl monzogranite	Qtz (31%), Kfs (31%), Pl (31%), Bt (6%), green Hbl (1%), Ms (s), Chl (s), Ttn (s), Prh (s), Opm (t), Zrn/Mnz (t), Aln (t), Ap (t)	inequigranular (fine- to medium-grained), hypidiomorphic, altered	G.H.I.C.	9.1
TAL58	337.19	subrounded	2.5x1.5x0.5	a) Bt orthogneiss	Qtz, Mc, Pl, Ms (s), Bt, Chl (s), Opm, Aln, Zrn/Mnz	heterogranular (fine- to medium-grained), gneissic texture (mm-scale compositional layering) with ribbon-like quartz aggregates, altered	K.G.	9.1
		angular	1.5x1x1	b) Bt-spotted schist	Qtz, Bt, Ms, Pl, Opm, Tur, Zrn/Mnz, Ap	heterogranular (very fine-grained to fine-grained), granolepidoblastic, Bt spots	S.G.?	9.1
TAL59	337.57	rounded	3.5x2x2	Gph-bearing marble	Cal, Opm, Qtz, Ms, Chl	heterogranular (fine-grained), compositional and grain-size layering, interlobate granoblastic	K.G.	9.1
TAL62	370.24	rounded	2.5x2.5x1	grey Bt-bearing monzogranite	Qtz (36%), Kfs (33%), Pl (31%), Bt (t), Ms (s), Chl (s), Prh (s), Opm (t), Zrn/Mnz (t), Ap (t)	equigranular (medium-grained), hypidiomorphic, altered	G.H.I.C.	9.1

dolerites are ubiquitous, with dolerite persistently forming the dominant lithology throughout the core and showing maximum abundance across the lithological boundary between LSU 7.4 and 7.5, and at the base of LSU 12.5. In contrast, all other lithologies show a more restricted distribution. Volcanic and very fine-grained dolerite clasts are abundant and persistent in the upper 0-150 mbsf interval, but they form a sparse clast population below 150 mbsf, mostly occurring within LSU 8.1 and at the base of LSU 11.1, along with dominant amygdule-bearing altered basalts. Sedimentary clasts show a wider distribution and are significantly more abundant below 150 mbsf; together with dolerites, they represent the prevailing rock types in the lowermost 32 m of the sequence. Coal fragments are very rare in the upper 150 m of the cored succession with only one occurrence, detected at 43 mbsf (LSU 1.2). In contrast, coal is persistently present from 159 mbsf downcore, and very abundant particularly in LSU 7.1 and in the lower part of LSU 12.5. Metamorphic rocks are definitely the least

abundant of all represented lithologies and form scattered occurrences throughout the core. Two major lithological variations can be highlighted: i) at *c.* 150 mbsf, marking the first appearance downward of abundant sedimentary clasts and concomitant decrease in the content of volcanic and/or very fine grained dolerite; and ii) at *c.* 791 mbsf, marking the upper boundary of a petrofacies assemblage confined to the lowermost *c.* 32 thick section, where dolerite forms almost 100% of the clasts, with very rare occurrences of granite and sedimentary (mainly Beacon arenite) clasts.

## PETROGRAPHICAL FEATURES AND MINERAL CHEMISTRY

### PETROGRAPHY

The main petrographical characteristics of the most common basement lithologies which form the pebble- to cobble-grain size fraction in the CRP-3

Tab. 1 - Continued.

Sample code	Top (mbsf)	Clast shape	Approximate size (cm)	Lithology	Mineral assemblage	Main petrographical features	Inferred provenance	LSU
TAL75	442.79	rounded	2.5x2x1	Bt-bearing meta-sandstone	Qtz, Pl, Ms, Bt, Chl (s), Opm	equigranular (fine-grained), granolepidoblastic, Bt spots	S.G./B.S.? (contact metamorphosed?)	11.1
TAL78	482.53	subangular	1x1.5x0.5	grey Bt monzogranite	Mc (36%), Qtz (34%), Pl (28%), Bt (2%), Ms (s), Chl (s), Cal (s), Opm (t), Rt (s), Ap (t), Zrn/Mnz (t)	inequigranular (fine- to medium-grained), hypidiomorphic, altered	G.H.I.C.	12.3
TAL79	488.61	subangular	1x0.5x0.5	grey Bt monzogranite	Qtz (35%), Pl (32%), Kfs (30%), Bt (3%), Ms (s), Chl (s), Opm (t), Ttn (s), Aln (t), Ap (t), Zrn/Mnz (t)	equigranular (medium-grained), hypidiomorphic, altered	G.H.I.C.	12.3
TAL83	554.70	subrounded	1.5x1x1	Sil-Bt paragneiss	Qtz, Bt, Pl, Kfs, Sil, Ms (s), Opm, Zrn/Mnz, Tur, Ap	equigranular (fine-grained), granolepidoblastic	K.G.	12.4
TAL84	561.54	subangular	2.5x1.5x0.5	black Bt-Cal-Czo meta-siltstone	Qtz, Pl, Bt, Ms, Cal, Czo, Opm, Tur	equigranular (very fine-grained), compositional layering, interlobate granolepidoblastic	S.G./B.S.? (contact metamorphosed?)	12.5
TAL85	561.91	subrounded	6x4.5x2	pink Bt monzogranite	Qtz (35%), Pl (33%), Kfs (25%), Bt (7%), Ms (s), Chl (s), Rt (s), Opm (t), Zrn/Mnz (t)	equigranular (fine-grained), hypidiomorphic, slightly altered	G.H.I.C.	12.5
TAL92	605.77	subangular	1x0.5x0.5	microgranite	Qtz (50%), Ms (s), Pl (30%), Kfs (20%), Chl (s), Opm (t), Zrn/Mnz (t)	equigranular (fine-grained), allotriomorphic, strongly altered	G.H.I.C.	12.6
TAL97	628.06	subangular	1x0.5x0.5	foliated Bt leucomonzogranite	Qtz (37%), Pl (35%), Mc (27%), Bt (1%), Ms (s), Chl (s), Ttn (s), Prh (s), Opm (t)	inequigranular (fine- to medium-grained), gneissic texture with mm-sized feldspar porphyroclasts and quartz ribbons, strongly altered	G.H.I.C.	13.1
TAL98	628.69	rounded	0.5x1x1	Cal-Bt meta-marl	Qtz, Fds, Cal, Bt, Ms, Opm, Zrn/Mnz, Tur	equigranular (fine-grained), compositional layering, lepidogranoblastic	S.G./B.S.? (contact metamorphosed?)	13.1
TAL100	644.50	rounded	1.5x1x0.5	Bt orthogneiss	Qtz, Pl, Kfs, Bt, Ms (s), Ttn (s), Opm, Zrn/Mnz	heterogranular (fine- to medium-grained), interlobate granoblastic and quartz ribbons	K.G.	13.1
TAL103	675.63	subrounded	1.5x1x0.5	foliated grey Bt-bearing monzogranite	Qtz (40%), Pl (38%), Kfs (20%), Bt (2%), Ms (s), Chl (s), Opm (t), Ttn (s), Zrn/Mnz (t)	equigranular (fine-grained), allotriomorphic, sub-solidus deformational microstructures, slightly altered	G.H.I.C.	13.1
TAL109	713.29	subrounded	2x1x1	Bt-Hbl monzogranite	Qtz (33%), Mc (33%), Pl (31%), Bt (2%), green Hbl (1%), Ms (s), Ep (s), Chl (s), Ttn (s), Opm (t), Zrn/Mnz (t)	inequigranular (fine- to medium-grained), hypidiomorphic, strongly altered	G.H.I.C.	13.1
TAL110	734.67	angular	1.5x0.5x0.5	layered Bt-Cam meta-marl	Qtz, Cal, Fds, Bt, Cam, Opm, Tur, Zrn/Mnz	heterogranular (very fine- to fine grained), compositional and grain-size layering, granoblastic Cal-rich layers, lepidogranoblastic Bt-rich layers	S.G./B.S.? (contact metamorphosed?)	13.1
TAL112	738.45	angular	4x2x1.5	pink Bt-Hbl monzogranite	Qtz (30%), Mc (30%), Pl (30%), Bt (5%), green Hbl (5%), Ms (s), Chl (s), Cal (s), Ttn (s), Prh (s), Aln (t), Opm (t), Ap (t), Zrn/Mnz (t)	inequigranular (medium- to coarse-grained), hypidiomorphic, altered	G.H.I.C.	13.1
TAL113	756.16	subrounded	2x1.5x0.5	Bt-Cal-Cam meta-feldspathic arenite	Qtz, Pl, Bt, Cal, Cam, Ms, Chl (s), Opm, Ttn, Zrn/Mnz	heterogranular (fine- to very fine-grained), compositional layering, interlobate lepidogranoblastic	S.G./B.S.? (contact metamorphosed?)	13.1
TAL118	774.96	subrounded	2x1x1	Bt meta-sandstone	Qtz, Pl, Bt, Ms, Chl (s), Opm, Ap, Zrn/Mnz	equigranular (fine-grained), interlobate lepidogranoblastic	S.G./B.S.? (contact metamorphosed?)	13.2
TAL119	781.93	subrounded	4x3x2	Bt meta-sandstone	Qtz, Pl, Bt, Cal, Chl (s), Ms (s), Opm, Ttn (s), Zrn/Mnz	equigranular (fine-grained), interlobate granoblastic	B.S.? (contact metamorphosed?)	13.2
TAL121	785.56	subangular	7x2x2	Bt-Hbl quartz-monzonitic porphyry	Pl (40%), Kfs (27%), Qtz (18%), Bt (10%), green/brown Hbl (5%), Ms (s), Chl (s), Ttn (s), Cal (s), Opm (t), Aln (t), Zrn/Mnz (t)	inequigranular (fine- to medium-grained), porphyritic, feldspar phenocrysts set within a Qtz-Kfs granophyric groundmass, altered	G.H.I.C.	13.2
TAL125	815.23	rounded	1x1x0.5	grey Bt monzogranite	Pl (35%), Kfs (33%), Qtz (31%), Bt (1%), Ms (s), Chl (s), Ep (s), Opm (s), Ap (t), Zrn/Mnz (t)	equigranular (medium-grained), hypidiomorphic, altered	G.H.I.C.	15.2

Notes: mineral abbreviations are according to Kretz (1983); with the addition of Opm to indicate opaque minerals). Modal contents of essential phases for magmatic rocks are given as percentages. t: trace (<1% modal content), s: mineral phase of secondary origin. Lithostratigraphic sub-Unit (LSU) designation from Cape Roberts Science Team (2000).

B.S. = Beacon Supergroup; G.H.I.C. = Granite Harbour Intrusive Complex; K.G. = Koettlitz Group; S.G. = Skelton Group.

core are here described. Representative samples to show the lithological range and the mineral assemblages typical of most common basement clasts throughout the borehole are listed in table 1. The table includes information on the lithology, the most relevant petrographical features, the most likely source-rock units in the crystalline basement of South Victoria Land, and the stratigraphical position in the CRP-3 core.

Like CRP-1 and CRP-2/2A basement clasts, most samples show a variably developed, but commonly extensive alteration. This affected the primary mineral assemblages through static, strain-free transformations (pseudomorphs and reaction rims), which occurred under low temperature, greenschist to sub-greenschist facies conditions. These mineral transformations include the partial to complete replacement of calcic plagioclase by saussurite (epidote + sericite  $\pm$  albite  $\pm$  calcite), the replacement of K-feldspar by sericite or kaolinite micro-aggregates (commonly more advanced in pink or red-coloured granitoids and porphyry than in the grey varieties), the partial replacement of hornblende by actinolite and/or chlorite, and the extensive alteration of red-brown biotite into Fe-Mg or Mg-Fe chlorite and/or prehnite + titanite  $\pm$  opaque minerals.

The main lithological types can be divided into two major groups: granitoids and less common metamorphic rocks. Granitoid pebbles consist of dominant grey biotite-bearing monzogranite, pink biotite-hornblende monzogranite and biotite-bearing leucomonzogranite. Minor varieties include: actinolite-bearing leucotonalite, microgranite, biotite-hornblende quartz-monzonitic porphyry, and foliated biotite leucomonzogranite.

Metamorphic clasts include rocks of both granitic and sedimentary derivation. They include: mylonitic biotite orthogneiss, with or without garnet, muscovite-bearing quartzite, sillimanite-biotite paragneiss, biotite meta-sandstone, biotite-spotted schist, biotite-calcite-clinoamphibole meta-feldspathic arenite, biotite-calcite-clinozoisite meta-siltstone, biotite-clinoamphibole meta-marl, and graphite-bearing marble.

*Grey and pink biotite  $\pm$  hornblende monzogranites* (30.61, 43.57, 107.32, 168.73, 176.03, 178.41, 216.98, 256.38, 335.31, 370.24, 482.53, 488.61, 561.91, 713.29, 738.45, 815.23 mbsf) are commonly inequigranular (fine- to medium/coarse-grained) and hypidiomorphic, except for sample TAL26, which shows a porphyritic texture. Alkali feldspar is microperthitic orthoclase or microcline, often occurring as anhedral phenocrysts and transformed into a felty micro-aggregate of kaolinite or sericite. Plagioclase (oligoclase-andesine) forms subhedral to euhedral laths that commonly show a marked normal compositional zoning and are mostly transformed into sericite or saussurite. Red-brown biotite is in places intergrown with euhedral crystals of green hornblende and it is partly replaced by FeMg-chlorite

$\pm$ prehnite  $\pm$ titanite  $\pm$ epidote. Typical accessory phases include opaque minerals (commonly ilmenite), apatite, monazite/zircon and allanite.

*Foliated biotite-bearing leucomonzogranites* (628.06, 675.63 mbsf) are characterized by similar mineral assemblages as the monzogranites, but their fabrics show a number of features, such as subgrain boundaries, wavy extinction, kink-bands, deformation twins and a weak to marked foliation defined by recrystallized feldspars and biotite, which are indicative of solid-state deformation.

*Actinolite-bearing leucotonalite* (50.25 mbsf) is inequigranular, medium- to fine-grained, and hypidiomorphic. Euhedral plagioclase laths (andesine) show compositional patch zoning and are almost completely replaced by saussurite. Quartz is interstitial with plagioclase and is associated with subhedral crystals of actinolite, replaced by FeMg-chlorite and opaque minerals.

*Biotite-hornblende quartz-monzonitic porphyry* (785.56 mbsf) consists of idiomorphic phenocrysts of andesine (normally zoned and sericitized) and orthoclase (microperthitic and replaced by clay mineral micro-aggregates or sericite) set within a fine-grained granophyric groundmass consisting of Kfeldspar-quartz intergrowths and oligoclase associated with aggregates of red-brown biotite and euhedral crystals of hornblende (brown cores, green rims). Accessory phases consist of opaque minerals, allanite and zircon/monazite. A quartz-dioritic *enclave* has a similar porphyritic texture (plagioclase phenocrysts set in a fine-grained subophitic groundmass consisting of plagioclase, quartz and green hornblende).

*Microgranite* (605.77 mbsf) is equigranular, fine grained and allotriomorphic and consists of anhedral crystals of quartz and feldspars completely replaced by muscovite, and scattered flakes of biotite, transformed to chlorite. Accessory phases include opaque minerals and zircon/monazite.

*Mylonitic biotite with or without garnet orthogneisses* (166.18, 231.78, 337.19, 644.50 mbsf) are fine- to medium-grained and commonly show a gneissic texture, with a mm-scale compositional layering composed of interlobate granoblastic layers of quartz or quartz and feldspars, sometimes characterized by the presence of mm-sized feldspar porphyroclasts. Feldspars (microcline and oligoclase) are present both as xenoblastic and elongated crystals and are partly replaced by sericite. Biotite occurs as tiny disorientated aggregates, and garnet (only found in sample TAL22) as idiomorphs within quartz-feldspar layers.

*Muscovite-bearing quartzite* (132.19 mbsf) has an equigranular (fine-grained) subpolygonal granoblastic texture and consists mainly of quartz associated with tiny flakes of muscovite whose alignment defines a slight foliation. Accessory phases are represented by green tourmaline (forming small subidioblastic

grains), opaque minerals and zircon/monazite.

*Sillimanite-biotite paragneiss* (554.70 mbsf) is equigranular fine-grained and has a granolepidoblastic texture. Quartz, K-feldspar and andesine consist of xenoblasts associated with aggregates of biotite flakes and prismatic idioblasts of sillimanite. Muscovite only occurs as a secondary phase after feldspars.

*Biotite meta-sandstones* and *meta-quartz arenite* (227.98, 442.79, 774.96, 781.93 mbsf) have an equigranular fine-grained interlobate granoblastic to granolepidoblastic texture and consist of quartz and plagioclase (in variable proportions) associated with muscovite and biotite flakes. Rarely, calcite is present interstitial to quartz and plagioclase.

*Biotite-spotted schist* (337.19 mbsf) has a similar mineralogical assemblage to the previous lithology but biotite is more widespread and also occurs as rounded mm-sized porphyroblasts. Common accessory phases are opaque minerals and green tourmaline.

*Biotite-calcite-clinoamphibole meta-feldspathic arenite* (756.16 mbsf) is heterogranular (fine- to very fine-grained) granolepidoblastic, and consists of xenoblasts of quartz and plagioclase (labradorite) with interstitial calcite, tiny isorientated flakes of biotite and muscovite, and xenomorphic actinolitic clinoamphibole. A mm-scale compositional layering is present.

*Biotite-calcite-clinozoisite meta-siltstone* (561.54 mbsf) has a very fine grain size and consists of an interlobate granolepidoblastic association of quartz, plagioclase, calcite, biotite, muscovite and clinozoisite. The presence of opaque minerals and biotite-rich layers is responsible for the compositional layering.

*Biotite±clinoamphibole meta-marls* (628.69, 734.67 mbsf) are fine-grained and characterized by a compositional and textural layering consisting of interlobate to subpolygonal granoblastic calcite-rich or

quartz-feldspar layers alternating with granolepidoblastic biotite-muscovite-rich layers. Actinolitic clinoamphibole occurs only in one sample (TAL110) within the mica-rich layers.

*Graphite-bearing marble* (337.57 mbsf) is heterogranular (fine-grained) interlobate granoblastic and has a compositional and grain-size layering composed of calcite layers alternating with graphite-rich calcite layers or lenses, characterized by a relatively finer grain size. Scattered muscovite and chlorite flakes usually occur within the graphite-rich layers.

#### MINERAL CHEMISTRY

Ten samples (5 magmatic and 5 metamorphic rocks) were selected for mineral analysis: biotite monzogranite (TAL23), foliated biotite monzogranite (TAL103), undeformed biotite-hornblende monzogranite (TAL43 and TAL26), biotite-hornblende quartz-monzonitic porphyry (TAL121), biotite orthogneiss with (TAL22) and without garnet (TAL58a), sillimanite-biotite paragneiss (TAL83), biotite-spotted schist (TAL58b) and biotite-calcite-clinoamphibole meta-feldspathic arenite (TAL113) (Tab. 1).

Chemical analyses of the main mineral phases were carried out with an energy-dispersive X-ray system (EDAX DX4) attached to a Scansion Electron Microscope (Philips XL30), at 20 kV, 60 µA of beam current and beam spot size of 2 µm, using natural minerals as standards. Fe<sub>2</sub>O<sub>3</sub> in clinoamphiboles was calculated assuming charge balance and the equation given by Papike et al. (1974).

*Biotite* - Representative compositions are listed in table 2. No significant intra-crystalline compositional zoning was detected. In the monzogranites (TAL23, TAL103, TAL43, TAL26), biotite composition is

Tab. 2 - Representative chemical analyses of biotite in CRP-3 basement clasts.

Oxide (wt%)	TAL23	TAL103	TAL43	TAL26	TAL121	TAL22	TAL58a	TAL83	TAL58b	TAL113						
SiO <sub>2</sub>	35.92	36.02	35.77	35.68	34.40	34.54	36.34	35.76	34.85	34.02	34.61	37.73	37.14	38.46	37.14	37.71
Al <sub>2</sub> O <sub>3</sub>	15.51	15.53	16.61	16.55	13.72	13.48	12.72	14.00	14.39	17.50	17.91	16.13	19.86	19.34	18.08	17.01
TiO <sub>2</sub>	2.32	2.26	2.26	3.05	4.29	4.58	4.03	4.64	4.79	3.28	2.87	1.61	2.60	1.53	2.26	2.54
MgO	2.44	2.48	6.90	6.89	5.29	5.22	7.93	7.08	6.16	6.09	6.35	13.38	10.00	13.84	12.63	12.56
FeO	31.14	31.15	25.23	24.61	30.52	29.91	26.67	25.99	27.58	28.13	26.58	17.72	17.39	14.32	16.70	17.28
MnO	0.24	0.18	0.38	0.41	0.41	0.30	0.14	0.10	0.21	0.34	0.27	0.14	0.20	0.00	0.19	0.08
K <sub>2</sub> O	8.62	8.60	0.04	0.00	0.00	0.00	0.00	0.00	0.00	0.33	0.00	0.00	0.00	0.00	0.00	0.00
Na <sub>2</sub> O	0.39	0.37	0.56	0.44	0.34	0.44	0.53	0.55	0.51	0.58	0.49	0.50	0.41	0.55	0.49	0.52
CaO	0.00	0.00	8.76	8.83	7.81	8.08	8.51	8.36	8.25	6.12	7.32	9.25	8.88	8.44	9.16	8.84
Total	96.58	96.59	96.50	96.47	96.78	96.54	96.87	96.47	96.75	96.38	96.42	96.47	96.47	96.48	96.67	96.54
Structural formulae on the basis of 22 oxygens																
Si	5.71	5.72	5.54	5.51	5.46	5.49	5.65	5.56	5.46	5.29	5.35	5.62	5.48	5.57	5.49	5.58
Al <sup>IV</sup>	2.29	2.28	2.46	2.49	2.54	2.51	2.33	2.44	2.54	2.71	2.65	2.38	2.52	2.43	2.51	2.42
Al <sup>VI</sup>	0.61	0.63	0.54	0.52	0.03	0.01	0.00	0.13	0.11	0.49	0.61	0.45	0.94	0.87	0.64	0.55
Ti	0.28	0.27	0.26	0.35	0.51	0.55	0.47	0.54	0.56	0.38	0.33	0.18	0.29	0.17	0.25	0.28
Mg	0.58	0.59	1.59	1.59	1.25	1.24	1.84	1.64	1.44	1.41	1.46	2.97	2.20	2.99	2.78	2.77
Fe	4.14	4.13	3.27	3.18	4.05	3.97	3.47	3.38	3.61	3.65	3.44	2.21	2.15	1.73	2.06	2.14
Mn	0.03	0.02	0.05	0.05	0.05	0.04	0.02	0.01	0.03	0.04	0.04	0.02	0.03	0.00	0.02	0.01
K	1.75	1.74	0.01	0.00	0.00	0.00	0.00	0.00	0.00	0.05	0.00	0.00	0.00	0.00	0.00	0.00
Na	0.12	0.11	0.17	0.13	0.10	0.14	0.16	0.17	0.16	0.17	0.15	0.14	0.12	0.15	0.14	0.15
Ca	0.00	0.00	1.73	1.74	1.58	1.64	1.69	1.66	1.65	1.21	1.44	1.76	1.67	1.56	1.73	1.67
Total	15.51	15.49	15.61	15.56	15.59	15.58	15.63	15.53	15.55	15.42	15.47	15.73	15.39	15.47	15.63	15.57
X <sub>Fe</sub>	0.88	0.88	0.67	0.67	0.76	0.76	0.65	0.67	0.72	0.72	0.70	0.43	0.49	0.37	0.43	0.44

Note: total Fe as FeO. X<sub>Fe</sub>=Fe/(Fe+Mg).

characterised by  $Al^{IV}$  from 2.28 to 2.54 (atoms *per* formula unit, a.p.f.u. on the basis of 22 oxygens) and  $X_{Fe}$  between 0.65 and 0.88 (Fig. 1); higher  $X_{Fe}$  values refer to biotite in undeformed monzogranite (TAL23), while the lower values are from porphyritic biotite-hornblende monzogranite (TAL26). Biotite-hornblende quartz-monzonitic porphyry (TAL121) shows an  $X_{Fe}$  ranging from 0.67 to 0.72, similar to the biotite-hornblende monzogranite values. In the  $FeO_{tot}$ - $MgO$ - $Al_2O_3$  diagram (Rossi & Chevremont, 1987; Fig. 2) most sample data fall in the Fe-potassic monzonitic field with the exception of sample TAL103, whose biotite data plot in the calcalkaline field. Biotite from orthogneisses has a quite different composition within the two varieties (with or without garnet):  $X_{Fe}$  is 0.42-0.43 in TAL58a and 0.70-0.72 in TAL22.  $X_{Fe}$  in sillimanite-biotite paragneiss (TAL83) shows a very limited compositional range between 0.49 and 0.50. Samples whose inferred provenance does not seem to be the Koettlitz Group (biotite-spotted schist TAL58b, and biotite-calcite-clinoamphibole meta-feldspathic arenite TAL113) have the lowest  $X_{Fe}$  values compared with all the other lithologies (0.36-0.37 and 0.42-0.44, respectively).

**Clinoamphibole** - Representative analyses are listed in table 3. In all samples, amphiboles are members of the calcic-amphibole group (Leake, 1978; Fig. 3), but in all the magmatic lithologies they show different  $(Na+K)_A$  values, both higher and lower than 0.50. Hornblende-biotite monzogranites (TAL43, TAL26) contain zoned amphiboles, ranging from Fe-tschermakitic hornblende ( $X_{Mg}=0.49-0.47$ , core) to Fe-hornblende or Fe-edenitic hornblende ( $X_{Mg}=0.31$ , rim). Biotite-hornblende quartz-monzonitic porphyry (TAL121) has amphiboles with a very marked zoning, characterized by cores of magnesian hastingsite or tschermakitic hornblende ( $X_{Mg}=0.71-0.59$ ) and rims of Fe-hornblende or Fe-edenitic hornblende ( $X_{Mg}=0.49-0.38$ ). Amphiboles from meta-feldspathic arenite (TAL113) are actinolitic or Mg-hornblende, with  $X_{Mg}$  ranging from 0.71 to 0.73.

**Garnet** - Garnets have been found in only one orthogneiss (TAL22), and their representative analyses are listed in table 3. They are almandines, with a very homogeneous composition and without intracrystalline zoning ( $alm_{72}prp_7sps_{17}grs_4$ ).

**Feldspars** - Representative compositions of plagioclase are listed in table 4. A weak to marked normal zoning was detected in plagioclase from all magmatic samples. In biotite monzogranites (TAL23, TAL103), plagioclase shows zonings ranging from  $an_{11-0}$  in the undeformed rock to  $an_{38-29}$  in the deformed one. In biotite-hornblende monzogranites (TAL43, TAL26), plagioclase has a more calcic composition (labradorite-andesine), and has a marked zoning ranging from  $an_{34}$  to  $an_{13}$  in TAL43 and from  $an_{60}$  to  $an_{30}$  in TAL26; the porphyritic sample (TAL26) has groundmass plagioclase of oligoclase composition ( $an_{24-26}$ ). Both porphyroclasts and newly

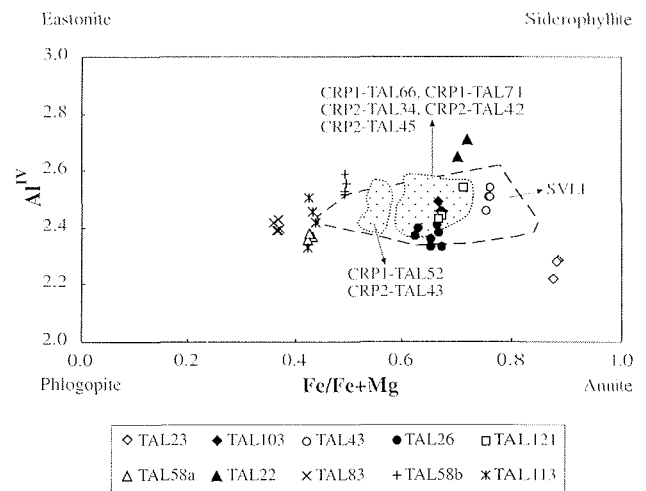


Fig. 1 - Biotite composition in terms of  $Al^{IV}$  vs  $Fe/(Fe+Mg)$  for CRP-3 basement clasts. Contoured field is that of biotite compositions from the calcalkaline South Victoria Land Intrusives (Armienti et al., 1990) on the basis of data reported in Biagini et al. (1991). Compositional fields of biotite from CRP-1 and CRP-2/2A basement clasts (Talarico & Sandroni, 1998; Talarico et al., 2000) are also shown for comparison.

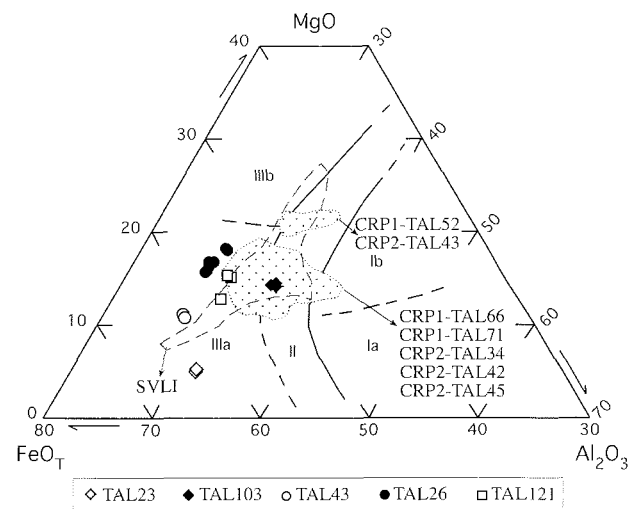


Fig. 2 - Ternary  $FeO_T$ - $MgO$ - $Al_2O_3$  diagram for biotites (after Rossi & Chevremont, 1987) from CRP-3 basement clasts. Field I: "aluminopotassique" association (Ia: type Limousine; Ib: type Guèret); field II: calcalkaline association; field III: monzonitic association (IIIa: Fe-potassic; IIIb: Mg-potassic). Outlined field is that of biotite compositions from the calcalkaline South Victoria Land Intrusives (Armienti et al., 1990) on the basis of data reported in Biagini et al. (1991). Compositional fields of biotite from CRP-1 and CRP-2/2A granitoid clasts (Talarico & Sandroni, 1998; Talarico et al., 2000) are also shown for comparison.

recrystallized grains from orthogneisses (TAL22, TAL58a) have a homogeneous oligoclase composition, ranging from  $an_{16}$  to  $an_{20}$ . Plagioclases from biotite-sillimanite paragneiss (TAL83) are also homogeneous, with an andesine composition ( $an_{33-38}$ ). Both biotite-spotted schist (TAL58b) and biotite-calcite-clinoamphibole meta-feldspathic arenite (TAL113) are characterized by zoning-free plagioclases, with a wide

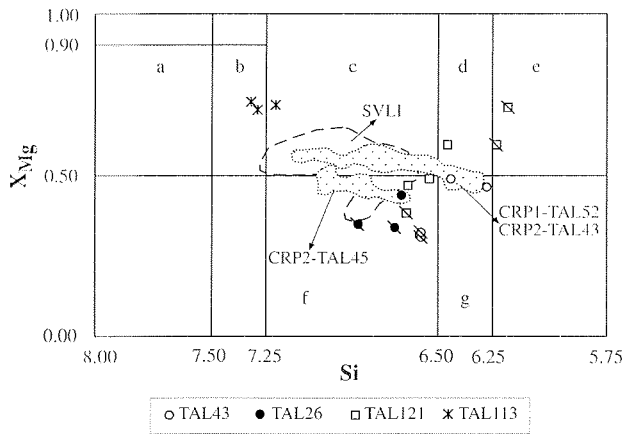


Fig. 3 - Calcic-amphiboles classification ((Ca+Na)<sub>B</sub>>1.34, Na<sub>B</sub><0.67, after Leake, 1978) for CRP-3 basement clasts. For samples with (Na+K)<sub>A</sub><0.50: a - actinolite; b - actinolitic hornblende; c - Mg-hornblende; d - tschermakitic hornblende; f - Fe-hornblende; g - Fe-tschermakitic hornblende. Stroked symbols represent compositions whose (Na+K)<sub>A</sub>>0.50; for those, compositional field names are: e - magnesian-hastingsite; f - Fe-edenitic hornblende. The contoured field is that of amphibole compositions from the calcalkaline South Victoria Land Intrusives (Armenti et al., 1990) on the basis of data reported in Biagini et al. (1991). Compositional fields of Ca-amphiboles from CRP-1 and CRP-2/2A basement clasts (Talarico & Sandroni, 1998; Talarico et al., 2000) are also shown for comparison.

compositional variation between each crystal: an<sub>32-55</sub> (andesine-labradorite) and an<sub>58-74</sub> (labradorite-bytownite), respectively.

Microperthitic K-feldspars from magmatic rock samples have an albite-rich bulk composition compared to the metamorphic ones. In biotite undeformed monzogranite (TAL23), K-feldspar shows a composition ranging from or<sub>52</sub> to or<sub>60</sub>, whereas in deformed monzogranite (TAL103) has a homogeneous and K-richer composition (or<sub>91-92</sub>). K-feldspar from hornblende-biotite monzogranites (TAL43, TAL26) ranges from or<sub>64</sub> to or<sub>87</sub>, usually with or-richer compositions for groundmass crystals. Granophytic K-feldspars from porphyry (TAL121) have an homogeneous or<sub>85</sub> bulk composition. Both porphyroclasts and groundmass K-feldspars from orthogneisses (TAL22, TAL58a) are homogeneous, with an or<sub>90-95</sub> composition. K-feldspar from biotite-sillimanite paragneiss (TAL83) is not microperthitic and has an or<sub>95</sub> composition.

**Tourmaline** - Tourmalines have been found only in metamorphic rock samples and all of them belong to the schorl-dravite series. In the orthogneiss (TAL22),

Tab. 3 - Representative chemical analyses of clin amphibole and garnet in CRP-3 basement clasts.

Oxide (wt%)	CLINOAMPHIBOLE								GARNET				
	TAL43		TAL26		TAL121		TAL113		TAL22		TAL22		
	1-c	1-r	1-c	1-r	1-c	1-r	1-c	1-r	1-c	1-r	1-c	1-r	
SiO <sub>2</sub>	42.71	41.45	42.17	41.96	42.75	43.98	43.58	43.67	43.11	50.94	50.43	37.84	37.89
Al <sub>2</sub> O <sub>3</sub>	10.04	10.39	9.19	9.49	8.21	7.74	9.87	8.24	8.85	6.65	6.89	20.80	20.94
TiO <sub>2</sub>	1.81	2.25	1.43	1.38	1.39	1.36	2.30	1.39	1.75	0.27	0.21	0.09	0.08
Fe <sub>2</sub> O <sub>3</sub>	8.03	8.28	0.65	0.36	0.26	8.83	6.90	7.05	0.11	3.29	4.59	0.00	0.00
MgO	7.94	7.50	6.28	6.23	6.98	7.30	10.17	8.10	7.99	13.75	13.75	1.67	1.55
FeO	14.84	15.41	25.17	25.08	24.77	16.68	12.44	16.60	22.96	10.12	9.35	30.44	30.59
MnO	0.24	0.29	0.39	0.27	0.44	0.43	0.11	0.16	0.22	0.43	0.48	7.27	7.32
CaO	10.29	10.34	10.25	10.31	10.17	10.11	10.78	10.68	10.48	11.70	11.72	1.33	1.26
Na <sub>2</sub> O	2.04	2.00	1.78	1.81	1.90	1.92	1.69	1.75	1.65	0.75	0.78	0.55	0.37
K <sub>2</sub> O	0.69	1.11	1.14	1.12	1.02	0.93	0.97	1.03	1.11	0.41	0.35	0.00	0.00
Total	98.65	99.03	98.46	98.01	97.87	99.29	98.81	98.66	98.22	98.33	98.56	99.99	100.00
Structural formulae on the basis of 23 oxygens,											12 oxygens		
Si	6.43	6.27	6.57	6.56	6.68	6.65	6.45	6.62	6.63	7.29	7.21	3.05	3.06
Al <sup>IV</sup>	1.57	1.73	1.43	1.44	1.32	1.35	1.55	1.38	1.37	0.71	0.79	0.00	0.00
Al <sup>VI</sup>	0.21	0.12	0.26	0.31	0.19	0.03	0.17	0.09	0.23	0.41	0.37	1.98	1.99
Ti	0.20	0.26	0.17	0.16	0.16	0.16	0.26	0.16	0.20	0.03	0.02	0.01	0.00
Fe <sup>2+</sup>	0.91	0.94	0.08	0.04	0.03	1.00	0.77	0.80	0.01	0.35	0.49	0.00	0.00
Mg	1.78	1.69	1.46	1.45	1.62	1.64	2.24	1.83	1.83	2.94	2.93	0.20	0.19
Fe <sup>3+</sup>	1.87	1.95	3.28	3.28	3.23	2.11	1.54	2.10	2.96	1.21	1.12	2.05	2.06
Mn	0.03	0.04	0.05	0.04	0.06	0.06	0.01	0.02	0.03	0.05	0.06	0.50	0.50
Ca	1.66	1.68	1.71	1.73	1.70	1.63	1.71	1.73	1.73	1.79	1.80	0.12	0.11
Na	0.60	0.59	0.54	0.55	0.57	0.56	0.48	0.51	0.49	0.21	0.22	0.09	0.06
K	0.13	0.21	0.23	0.22	0.20	0.18	0.18	0.20	0.22	0.08	0.06	0.00	0.00
Total	15.39	15.47	15.77	15.78	15.78	15.37	15.37	15.45	15.70	15.07	15.07	8.00	7.97
X <sub>Mg</sub>	0.49	0.46	0.31	0.31	0.33	0.44	0.59	0.47	0.38	0.71	0.72	-	-
prp	-	-	-	-	-	-	-	-	-	-	-	7	7
alm	-	-	-	-	-	-	-	-	-	-	-	72	72
sps	-	-	-	-	-	-	-	-	-	-	-	17	17
grs	-	-	-	-	-	-	-	-	-	-	-	4	4

Note: c - core composition; r - rim composition; X<sub>Mg</sub>=Mg/(Fe+Mg); prp=Mg/(Mg+Fe+Mn+Ca)x100; alm=Fe/(Mg+Fe+Mn+Ca)x100; sps=Mn/(Mg+Fe+Mn+Ca)x100; grs=Ca/(Mg+Fe+Mn+Ca)x100.

Tab. 4 - Representative plagioclase compositions in CRP-3 basement clasts.

	TAL23				TAL103		TAL26				TAL43		TAL121		TAL22	TAL58a	TAL58b	TAL113	TAL83
	1-c	1-r	2-c	2-r	1-c	1-r	1-c	1-r	1-r	2-g	1-c	1-r	1-c	1-r					
ab	88	99	88	96	60	69	38	56	66	73	63	84	50	64	83	79	45	35	61
an	11	0	11	3	38	29	60	42	30	26	34	13	47	33	16	20	55	64	38
or	1	1	1	1	2	2	2	2	4	1	3	3	3	3	1	1	0	1	1

Note: c - core composition; r - rim composition; g - groundmass crystals; ab=Na/(Na+Ca+K)x100; an=Ca/(Na+Ca+K)x100; or=K/(Na+Ca+K)x100.

tourmaline has  $X_{Mg}$  (Mg/Mg+Fe) ranging around 0.30 and  $X_{Ca}$  (Ca/Ca+Na) ranging from 0.15 to 0.18, whereas in schist (TAL58b) and paragneiss (TAL83) it has a magnesium- and calcium-richer composition ( $X_{Mg}$ =0.61 and 0.64, and  $X_{Ca}$ =0.27 and 0.30, respectively).

### COMPARISONS WITH ON-SHORE BASEMENT ROCK UNITS

Similar to previous drillholes (MSSTS-1, CIROS-1, CRP-1, CRP-2/2A) in the Neogene-Palaeogene sedimentary sequences of the McMurdo Sound (George, 1989; Barrett et al., 1986; Hambrey et al., 1989; Cape Roberts Science Team, 1998a, 1998d; Talarico & Sandroni, 1998; Talarico et al., 2000), the CRP-3 borehole provides further evidence for a varied provenance that closely mirrors the present-day on-shore locally exposed geological units. These include: 1) a late Precambrian-Early Palaeozoic basement (mainly Cambro-Ordovician granitoids and Precambrian medium- to high-grade metasediments); 2) quartz arenites, minor black siltstones and coal-bearing strata of the Devonian-Triassic Beacon Supergroup; and 3) dolerite sills and lavas (Kirkpatrick Basalt) of the Jurassic Ferrar Supergroup.

Consistent with preliminary petrographical results (Cape Roberts Science Team, 2000), the new petrographical and mineral chemistry data provide clear evidence that most of the basement-derived pebbles were supplied by the Granite Harbour Intrusive Complex (*i.e.* the most extensively exposed rock unit in the on-shore region; Gunn & Warren, 1962; Allibone et al., 1993a, 1993b; Turnbull et al., 1994).

Similar to CRP-1 and CRP-2/2A, the ubiquitous occurrence of undeformed biotite±hornblende monzogranite pebbles throughout the core closely mirrors the dominance of these rock types in the on-shore basement. These lithologies are indeed comparable to the hornblende-biotite and biotite (hornblende-lacking) monzogranites included in the Dry Valleys 2 (DV2) and Dry Valleys 1b (DV1b) suites respectively, by Smillie (1992) and Allibone et al. (1993b). In particular, in the region closer to the CRP drillsites, biotite monzogranites have been reported as forming extensive outcrops at Gondola Ridge and in the St. Johns Range and are major

constituents of the DV1b - Suess and St. Johns plutons (Allibone et al., 1993b). Additionally, hornblende-biotite monzogranites are known to be the prevailing lithology at Granite Harbour (*e.g.* Lion Island; Graham & Palmer, 1987), as well as in the eastern St. Johns Range along the Wheeler Valley (the DV2 - discordant Swinford Pluton of Allibone et al., 1993a). These Authors interpreted both DV1a and possibly DV1b granitoids as possible correlatives of the South Victoria Land Intrusives (SVLI) (as defined by Armienti et al., 1990). Compositional data on biotite and hornblende from this metaluminous suite are available for the northermost segment (between Cape Irizar and the Priestley Glacier, northern Victoria Land; Biagini et al., 1991). As shown in figures 1 and 2, most of the biotite compositions of monzogranite (TAL23, TAL103, TAL43, TAL26) and quartz-monzonitic porphyry (TAL121) pebbles are mostly comparable to those typical of the SVLI. Similarly, most of the hornblende compositions plot close to the compositional fields of hornblende from the SVLI and from previous CRP-1 and CRP-2 samples (Fig. 3).

Other, impersistent and less common, granitoid varieties occurring as pebble-to-cobble-grade clasts in CRP-3 include biotite leucomonzogranite, actinolite-bearing leucotonalite, biotite-hornblende quartz-monzonitic porphyry, and microgranite. Petrographically comparable lithologies have been described as a subordinate proportion of the Granite Harbour Intrusive Complex of southern Victoria Land. Leucogranite and microgranite pebbles are petrographically similar to the leucocratic biotite granite dykes which extensively occur throughout the region (*e.g.* the occurrences reported by Allibone et al., 1993a, in the Wright Valley, or by Turnbull et al., 1994, at the eastern margin of the Wheeler Pluton adjacent to the Suess Pluton in the Clare Range). Tonalites are rare and their nearest outcrops to Cape Roberts are those reported by Smillie (1987) in the cliffs west of the Rhone Glacier (Taylor Valley). Moreover, tonalites have been found included in granodiorite cropping out at Mount Murray and Mount Gauss, south of Mawson Glacier (Skinner & Ricker, 1968). The pebble of monzonitic porphyry is likely to have been derived from the younger Vanda felsic porphyry dykes (Allibone et al., 1991), which form intense dike swarms throughout the Mackay Glacier-Askard Range region (Turnbull et al., 1994).

and in the Convoy Range, north of the Mackay Glacier (Pocknall et al., 1994).

Metamorphic rocks such as sillimanite-biotite paragneiss, muscovite-bearing quartzite, mylonitic biotite±garnet orthogneiss and graphite-bearing marble are also known to be common rock types in the medium- to high-grade Koettlitz Group which, south of Mackay Glacier in the St. Johns, Olympus and Clare Ranges, forms two NNW- to NW-striking belts, separated by younger granitoid intrusions (Grindley & Warren, 1964; Williams et al., 1971; Findlay et al., 1984; Allibone, 1992; Turnbull et al., 1994; Isaac et al., 1995). Petrographically similar orthogneiss types were also found in CRP-1 and in CRP-2/2A. CRP-3 is apparently devoid of Ca-silicate rocks, which were found to be relatively common in the two previous CRP drillholes. In contrast, clasts of contact-metamorphosed terrigenous-sedimentary rocks and of foliated low-grade metasediments are rather abundant, even if scattered throughout the core below c. 228 mbsf. The occurrence of biotite-spotted schist and low-grade meta-sandstone and meta-marl showing foliated fabrics (Tab. 1) are note worthy as the on-shore exposures of these rocks are very limited and restricted to areas between the Skelton and Koettlitz Glaciers, about 200 km south of the CRP-3 drillsite (Skelton Group; Grindley & Warren, 1964). The provenance and primary geological setting of contact-metamorphosed sedimentary rocks (meta-quartz arenite and meta-sandstone, Tab. 1) remain uncertain. Apart from the thermal-metamorphic overprint, these rocks show a broad lithological and petrographical similarity with comparable rock types occurring in the Beacon Supergroup. If this attribution is correct, the contact-metamorphic overprint could document the thermal and hydrothermal processes related to the emplacement and cooling of Ferrar Supergroup intrusive and sub-volcanic suites.

## CONCLUSIONS

Similar to previous drillholes (MSSTS-1, CIROS-1, CRP-1, CRP-2/2A) in the McMurdo Sound, CRP-3 borehole provides further evidence for a varied provenance that closely mirrors the present-day on-shore locally exposed rock units. Prominent among these are Late Precambrian-Early Palaeozoic granitoids and medium- to high-grade metasediments, as well as clasts derived from Devonian-Triassic Beacon Supergroup and Jurassic Ferrar Supergroup.

Both petrographical and mineral chemistry data consistently support a supply of the most abundant basement-derived pebbles (mainly biotite±hornblende monzogranite pebbles and ubiquitously distributed) from the Granite Harbour Intrusive Complex, which forms the most extensive outcrop of crystalline basement within the inland sector of the Transantarctic Mountains facing the CRP-3 area.

Other, impersistent and less common, granitoid pebble- to cobble-grade clasts (including biotite leucomonzogranite, actinolite-bearing leucotonalite, biotite-hornblende quartz-monzonitic porphyry, and microgranite) are petrographically comparable to lithologies which have been reported as minor constituents of the Granite Harbour Intrusive Complex in southern Victoria Land.

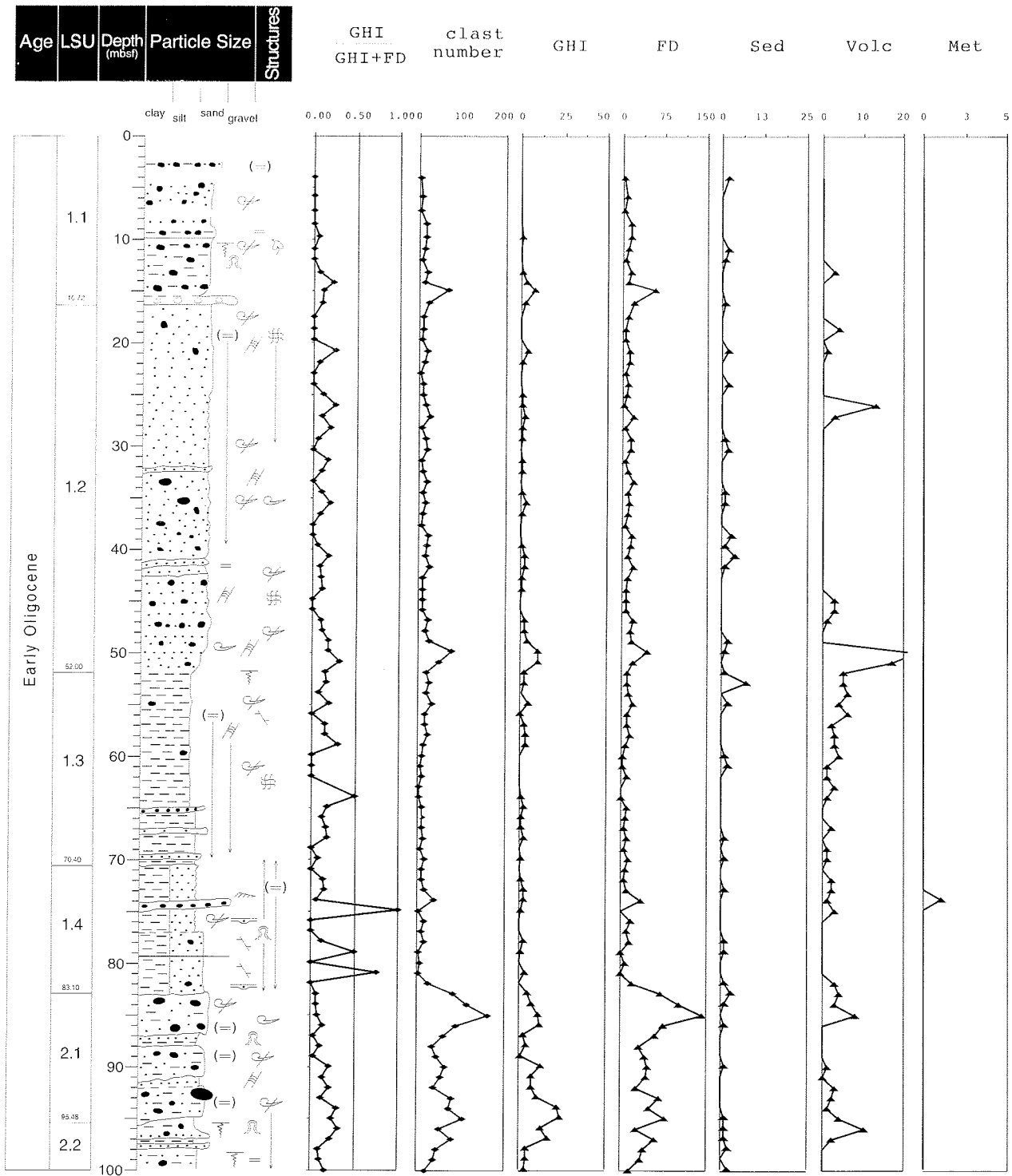
The most likely source for pebbles of sillimanite-biotite paragneiss, muscovite-bearing quartzite, mylonitic biotite±garnet orthogneiss and graphite-bearing marble, is identified with the medium- to high-grade Koettlitz Group, which forms a subordinate proportion of the pre-Devonian basement south of Mackay Glacier. Consistent with provenance information based on granitoid clasts, this correlation would further corroborate a model of local provenance for the supply of basement clasts in the CRP-3 strata. Nevertheless, the occurrence of scattered clasts of foliated low-grade metasediments suggests that the low-grade metamorphic terrain of the Skelton Group, which is restricted to the region between the Koettlitz and Skelton glaciers (about 200 km south of the CRP-3 drillsite), could also have contributed minor detritus to the CRP-3 sequence.

**ACKNOWLEDGMENTS** - We are grateful to J. Godge and D.N.B. Skinner for helpful reviews and improvements of the manuscript. This work was carried out as part of the Italian *Programma Nazionale di Ricerche in Antartide*. The Cape Roberts Project was made possible by the resources and close collaboration of the Antarctic programmes of Italy, New Zealand, United States of America, Germany, Australia, Great Britain and Holland, with field operation organized by Antarctica New Zealand. We wish to thank those involved in the field phase of the project for their efforts in recovering the core, and the International Steering Committee for access to the core material.

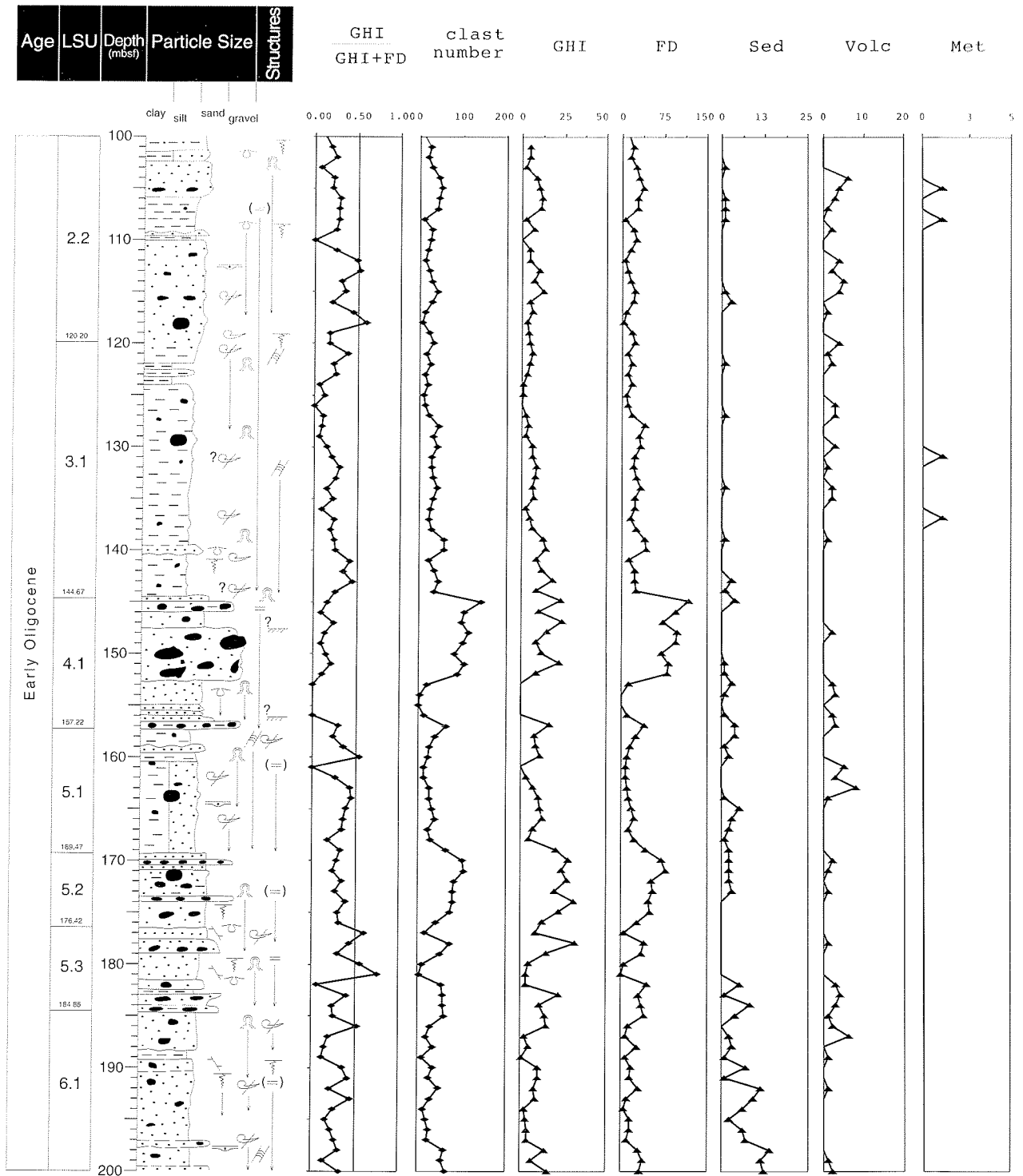
## REFERENCES

- Allibone A.H., 1992. Low pressure/high temperature metamorphism of Koettlitz Group schists in the Taylor Valley and Ferrar Glacier regions. *New Zealand Journal of Geology and Geophysics*, **35**, 115-127.
- Allibone A.H., Cox S.C., Graham I.J., Smillie R.W., Johnstone R.D., Ellery S.G. & Palmer K., 1993a. Granitoids of the Dry Valleys area, southern Victoria Land, Antarctica: field relationships, and isotopic dating. *New Zealand Journal of Geology and Geophysics*, **36**, 281-291.
- Allibone A.H., Cox S.C. & Smillie R.W., 1993b. Granitoids of the Dry Valleys area, southern Victoria Land: geochemistry and evolution along the early Palaeozoic Antarctic Craton margin. *New Zealand Journal of Geology and Geophysics*, **36**, 299-316.
- Allibone A.H., Forsyth P.J., Sewell R.J., Turnbull I.M. & Bradshaw M.A., 1991. Geology of the Thundergut area, southern Victoria Land, Antarctica, 1:50000. *New Zealand Geological Survey Miscellaneous Geological Map 21* (map and notes), Department of Scientific and Industrial Research, Wellington, New Zealand.
- Armienti P., Ghezzi C., Innocenti F., Manetti P., Rocchi S. & Tonarini S., 1990. Isotope geochemistry and petrology of

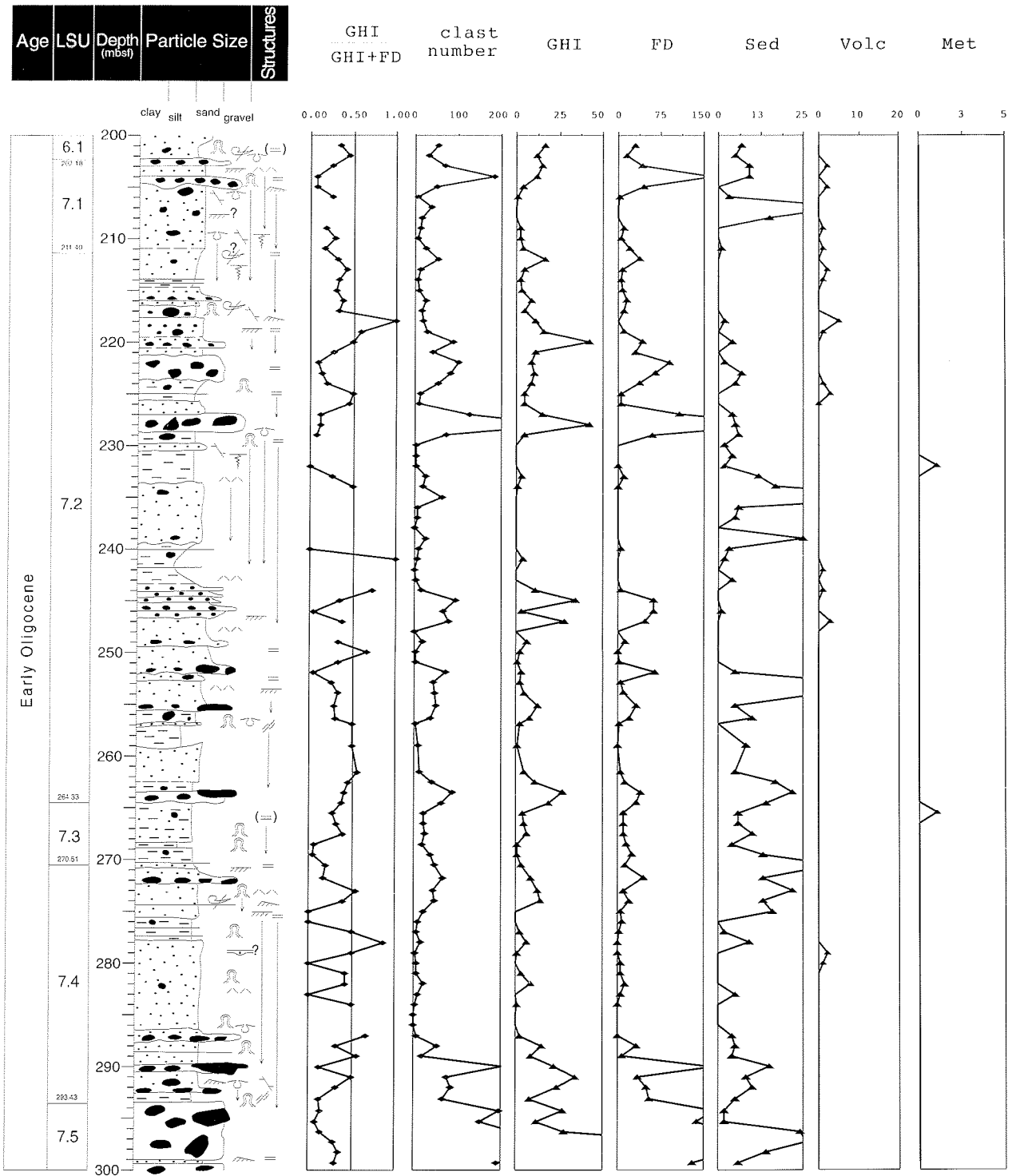
- granitoid suites from Granite Harbour Intrusives of the Wilson Terrane, north Victoria Land, Antarctica. *Eur. J. Mineral.*, **2**, 103-123.
- Barrett P.J., Elston D.P., Harwood D.M., McKelvey B.C. & Webb P.N., 1987. Mid-Cenozoic record of glaciation and sea level change on the margin of the Victoria Land basin, Antarctica. *Geology*, **15**, 634-637.
- Barrett P.J., McKelvey B.C. & Walker B.C., 1986. Sand provenance. *DSIR Bulletin*, **237**, 137-144.
- Biagini R., Di Vincenzo G. & Ghezzi C., 1991. Mineral chemistry of metalluminous granitoids between the David and Campbell Glaciers, Victoria Land (Antarctica). *Mem. Soc. Geol. It.*, **46**, 231-247.
- Cape Roberts Science Team, 1998a. Background to CRP-1, Cape Roberts Project, Antarctica. *Terra Antarctica*, **5**, 1-30.
- Cape Roberts Science Team, 1998b. Quaternary Strata in CRP-1, Cape Roberts Project, Antarctica. *Terra Antarctica*, **5**, 31-62.
- Cape Roberts Science Team, 1998c. Miocene Strata in CRP-1, Cape Roberts Project, Antarctica. *Terra Antarctica*, **5**, 63-124.
- Cape Roberts Science Team, 1998d. Summary Results from CRP-1, Cape Roberts Project, Antarctica. *Terra Antarctica*, **5**, 125-138.
- Cape Roberts Science Team, 2000. Studies from the Cape Roberts Project, Ross Sea, Antarctica. Initial Report on CRP-3. *Terra Antarctica*, **7**, 1-209.
- Cooper A.K., Brancolini G., Behrendt J.C., Davey F.J., Barrett P.J. & ANTOSTRAT Ross Sea Regional Working Group, 1994. A Record of Cenozoic Tectonism throughout the Ross Sea and Possible Controls on the Glacial Records. In: Cooper A.K., Barker P.F., Webb P.N. & Brancolini G. (eds.), *The Antarctic Continental Margin: Geophysical and Geological Stratigraphic Records of Cenozoic Glaciation, Palaeoenvironments, and Sea-Level Change*, *Terra Antarctica* **1**, 353-355.
- Findlay R.H., Skinner D.N.B. & Craw D., 1984. Lithostratigraphy and structure of the Koettlitz Group, McMurdo Sound, Antarctica. *New Zealand Journal of Geology and Geophysics*, **27**, 513-536.
- George A., 1989. Sand provenance. *DSIR Bulletin*, **245**, 159-167.
- Graham I.J. & Palmer K., 1987. New precise Rb-Sr mineral and whole-rock dates from I-type granitoids from Granite Harbour, south Victoria Land, Antarctica. *New Zealand Antarctic Record*, **8**, 72-80.
- Grindley G.W. & Warren G., 1964. Stratigraphic nomenclature and correlation in the western part of the Ross Sea. In: Adie R.J. (ed.), *Antarctic Geology*. Amsterdam, North Holland Publishing Co., 314-333.
- Gunn B.M. & Warren G., 1962. Geology of Victoria Land between the Mawson and Mulock Glaciers, Antarctica. *New Zealand Geological Survey Bulletin*, **71**.
- Hambrey M.J., Barrett P.J. & Robinson P.H., 1989. Stratigraphy. In: Barrett P.J. (ed.), *Antarctic Cenozoic history from the CIROS-1 drillhole, McMurdo Sound*, *DSIR Bulletin*, **245**, 23-48.
- Isaac M.J., Chinn T.J., Edbrooke S.W. & Forsyth P.J., 1995. Geology of the Olympus Range area, southern Victoria Land, Antarctica. Scale 1:50000. *Institute for Geological & Nuclear Sciences Geological Map 20*, 1 sheet, 60 p, Institute for Geological & Nuclear Sciences Ltd, Lower Hutt, New Zealand.
- Kretz R., 1983. Symbols for rock forming minerals. *Am. Mineral.*, **68**, 277-279.
- Leake B., 1978. Nomenclature of amphiboles. *Mineral. Petrogr. Acta*, **22**, 195-224.
- Papike J.J., Cameron K.L. & Baldwin K., 1974. Amphiboles and clinopyroxenes. Characterization of other than quadrilateral components and estimates of ferric iron from microprobe data. *Geol. Soc. Amer. Abstr. Programs*, **6**, 1053-1054.
- Pocknall D.T., Chinn T.J., Sykes R. & Skinner D.N.B., 1994. Geology of the Convoy Range area, southern Victoria Land, Antarctica. Scale 1:50000. *Institute for Geological & Nuclear Sciences Geological Map 11*, 1 sheet, 36 p, Institute for Geological & Nuclear Sciences Ltd, Lower Hutt, New Zealand.
- Pompilio M., Armienti P. & Tamponi M., 2001. Petrography, mineral composition and geochemistry of volcanic clasts from CRP-3, Victoria Land Basin, Antarctica. *This volume*.
- Rossi P. & Chevremont P., 1987. Classification des associations magmatiques granitoides. *Geochronique*, **21**, 14-18.
- Skinner D.N.B. & Ricker J., 1968. The geology of the region between the Mawson and Priestly glaciers, North Victoria Land, Antarctica, part II - Upper Palaeozoic to Quaternary geology. *N.Z. J. Geol. Geophys.*, **11**, 1041-1075.
- Smillie R.W., 1987. Petrological evolution of basement granitoids, southern Victoria Land. *New Zealand Antarctic Record*, **8**, 61-71.
- Smillie R.W., 1992. Suite subdivision and petrological evolution of granitoids from the Taylor Valley and Ferrar glacier region, south Victoria Land. *Antarctic Science*, **4**, 24, 71-87.
- Stump E., 1995. *The Ross Orogen of the Transantarctic Mountains*. Cambridge University Press, Cambridge, 284 p.
- Talarico F. & Sandroni S., 1998. Petrography, Mineral Chemistry and Provenance of Basement Clasts in the CRP-1 Drillcore (Victoria Land Basin, Antarctica). *Terra Antarctica*, **5**, 601-610.
- Talarico F., Sandroni S., Fielding C.R. & Atkins C., 2000. Variability, Petrography and Provenance of Basement Clasts from CRP-2/2A Drillcore (Victoria Land Basin, Ross Sea, Antarctica). *Terra Antarctica*, **7**, 529-544.
- Turnbull I.M., Allibone A.H., Forsyth P.J. & Heron D.W., 1994. Geology of the Bull Pass - St. Johns Range area, southern Victoria Land, Antarctica. Scale 1:50000. *Institute for Geological & Nuclear Sciences Geological Map 14*, 1 sheet, 52 p, Institute for Geological & Nuclear Sciences Ltd, Lower Hutt, New Zealand.
- Williams P.F., Hobbs B.E., Vernon R.H. & Anderson D.E. 1971. The structural and metamorphic geology of basement rocks in the McMurdo Sound area, Antarctica. *Journal of the Geological Society of Australia*, **18**, 127-142.



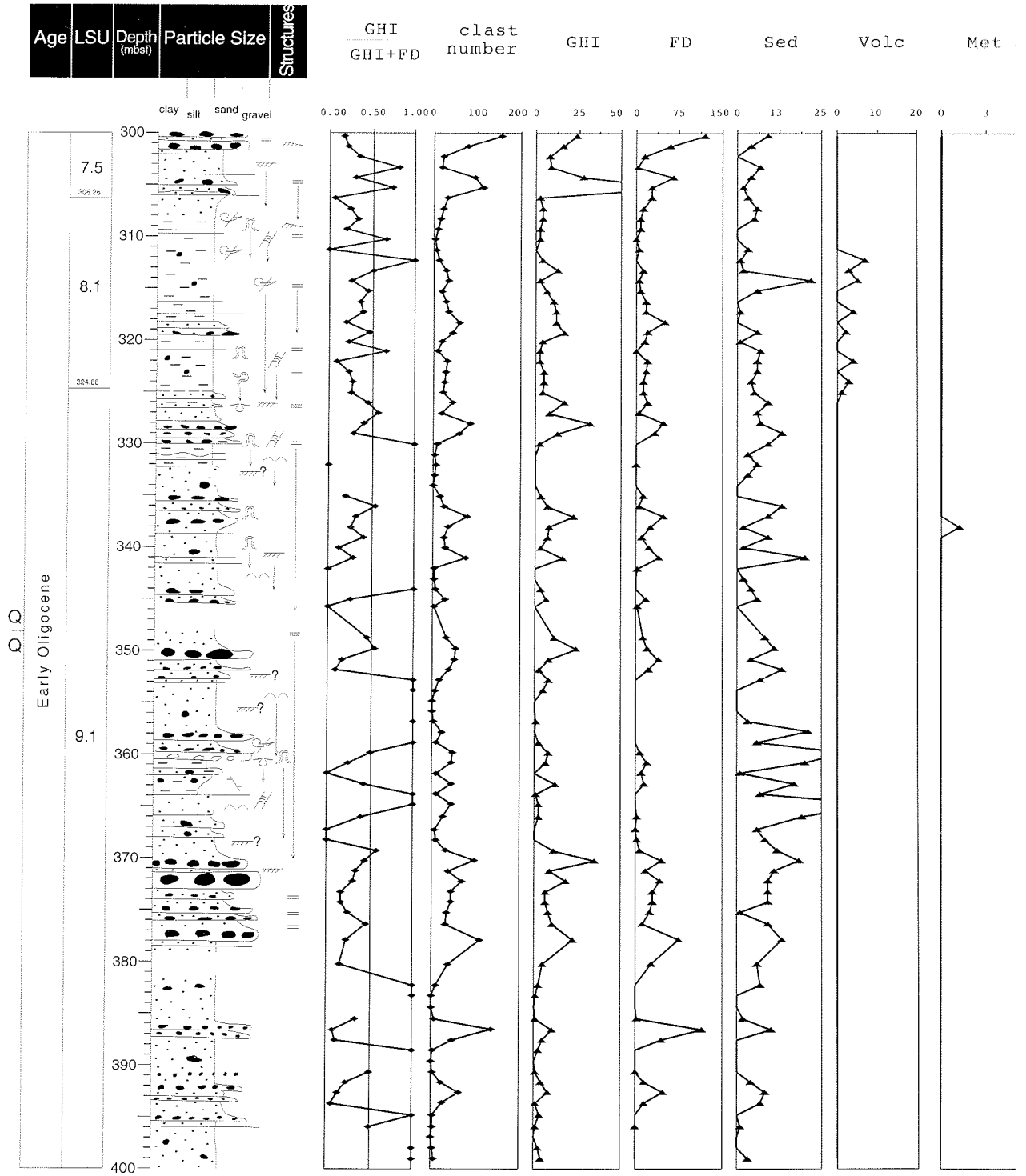
Appendix 1 - Distribution patterns of clasts (granule- to boulder-class) from CRP-3 drillcore. GHI: granitoids from the Granite Harbour Igneous Complex; FD: Ferrar dolerites; Sed: sedimentary clasts; Volc: volcanic and very fine grained dolerite clasts; Met: metamorphic clasts. GHI/GHI+FD: ratio between the number of granitoid clasts and the number of granitoid and dolerite clasts.



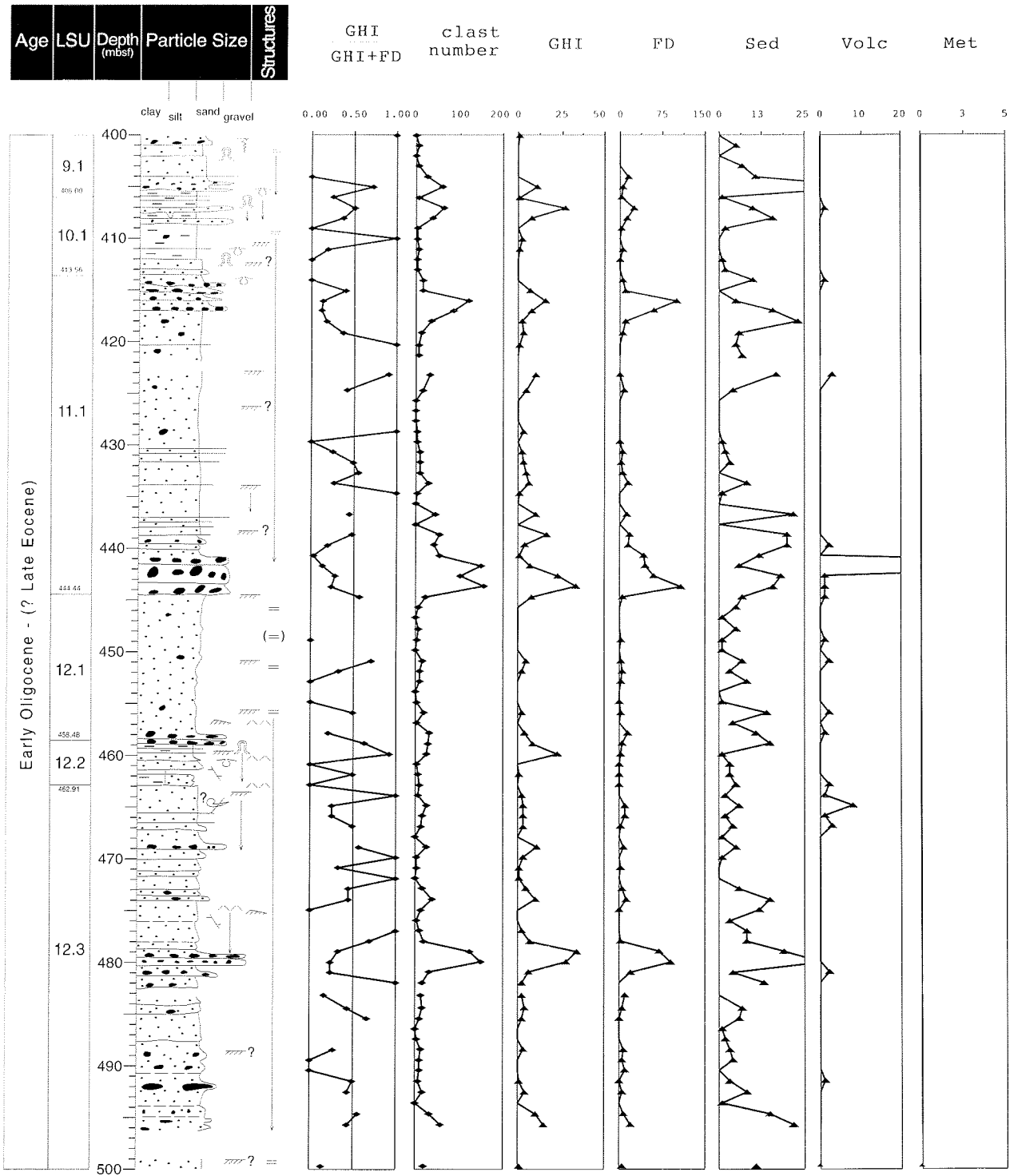
Appendix 1 - Continued.



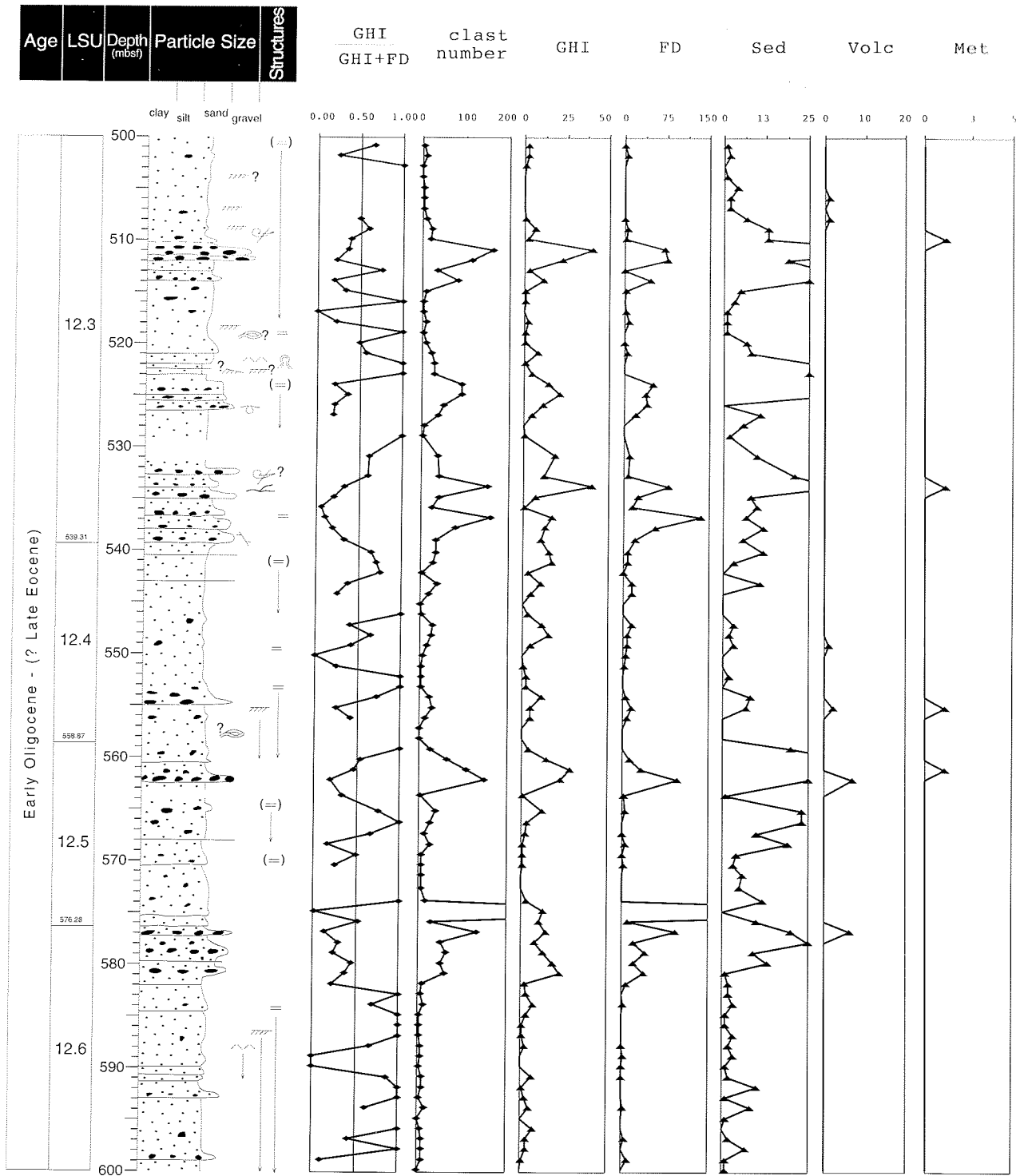
Appendix 1 - Continued.



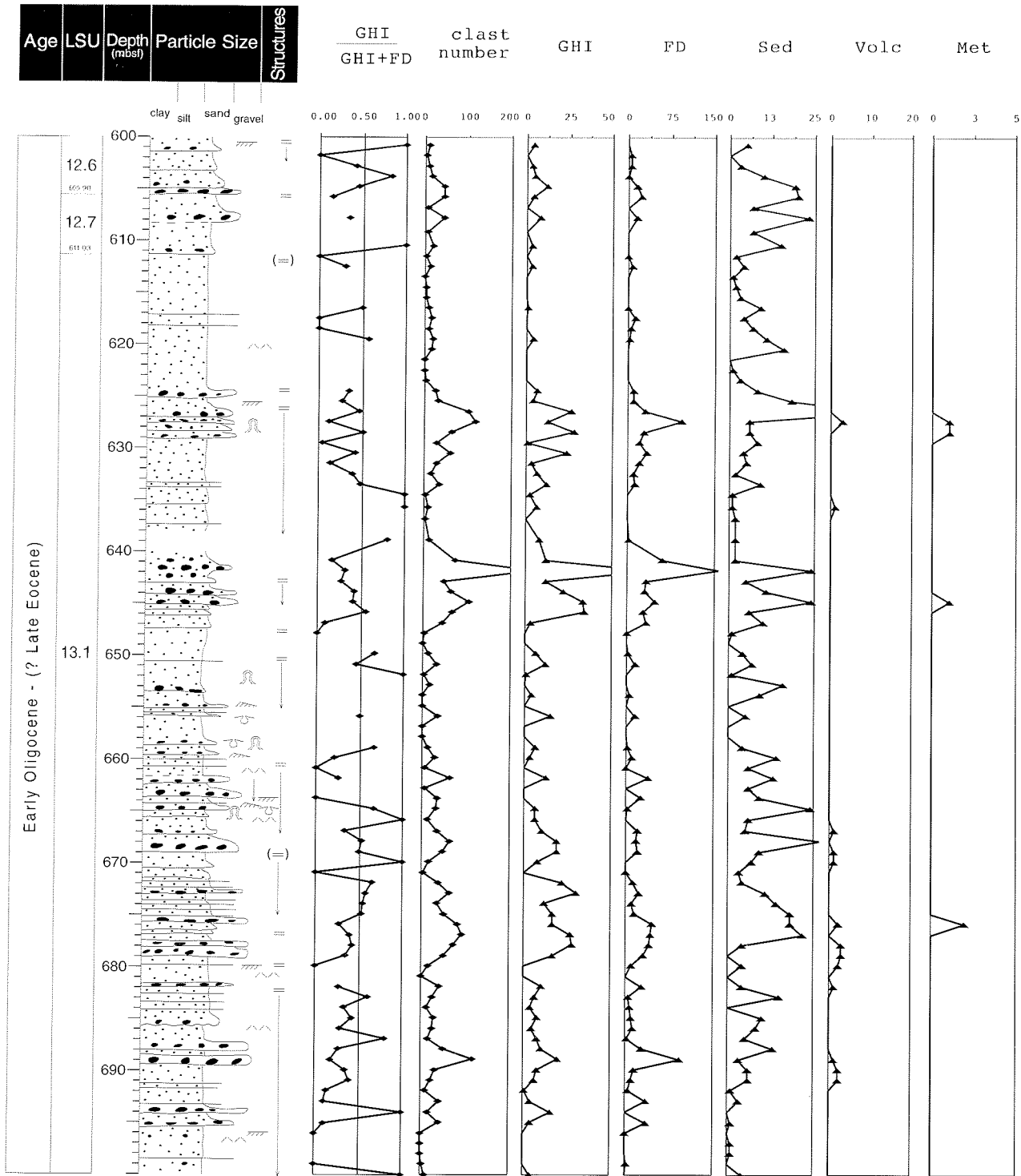
Appendix 1 - Continued.



Appendix 1 - Continued.



Appendix 1 - Continued.



Appendix 1 - Continued.